JOURNAL OF MATERIALS SCIENCE 18 (1983) 1917–1924

The segregation of calcium ions at the surface of magnesium oxide: theory and calculation

E. A. COLBOURN, W. C. MACKRODT
ICI PLC, New Science Group, PO Box 11, The Heath, Runcorn, Cheshire, UK
P. W. TASKER
Theoretical Physics Division, AERE Harwell, Oxon, UK

Atomistic simulation methods have been used to calculate the energetics of substitution and segregation of calcium ions near and at the {001} and {110} surfaces of magnesium oxide at thermal equilibrium. Defect clusters and complete planes of segregating ions have been considered, thereby including impurity–impurity interaction terms. Calculated enthalpies of segregation of −0.42 and −0.78 eV, derived from different interatomic potentials, are in good agreement with the experimental heat of segregation of −0.78 ± 0.22 eV reported recently by Wynblatt and McCune. A simple statistical mechanical theory leads to an Arrhenius expression for large crystals and the deviation from this behaviour expected in microcrystallites.

1. Introduction

Surfaces and interfaces in solids provide lattice defects, including impurities, with an environment which can differ markedly from that in the bulk. This difference is thought to lead to the formation of space-charge layers [1–3] and may also be responsible for gradients in impurity concentration [4–12], and stoichiometry [13–15], in the case of non-stoichiometric materials. All three are likely to affect crystal properties at thermal equilibrium. In particular, the segregation of impurity ions, which produces gradients in impurity concentration, can have an important influence not only on surface properties but on features such as bulk diffusion rates, even for crystals with the lowest levels of impurity. For more concentrated solid solutions of the type used to control material properties these effects are potentially even more significant. Many technological processes such as heterogeneous catalysis and corrosion are governed by surface structure and composition, most often of multi-component systems. A knowledge of equilibrium segregation, therefore, would seem to be an essential prerequisite for understanding and eventual control of these important processes.

Most studies of segregation have been concerned with metal surfaces and alloys [16]. Recently, however, experimental investigations have been reported for other materials, including the simpler oxides [4–12, 17, 18]. Sensitive surface techniques such as Auger electron spectroscopy (AES) and X-ray photoelectron spectroscopy (XPS) yield detailed measurements of surface composition, from the temperature dependence of which an effective enthalpy of segregation can be deduced [17]. However, here as elsewhere in materials science experimental difficulties can be severe and the interpretation of data prone to possible ambiguity. In these circumstances calculations of the type previously reported [19–23] might prove a useful adjunct to experiment. In a recent theoretical study the bulk and surface doping of MgO by several binary oxides has been examined using defect lattice methods [24]. There appears to be substantial agreement with such data as exist, but the neglect of impurity interaction effects in these calculations, strictly speaking, limits their range of validity to near infinite dilution. In view of the potential importance of segregation at higher levels of impurity we have chosen to study a single system, namely MgO–CaO, in rather greater detail than that given previously [24], and here report calculations

0022–2461/83 $03.00 + .12

based on a more complete atomistic approach which applies to finite dopant concentrations. In addition, we apply a simple statistical mechanical model that can be generalized to systems with more than two components. Finally we present modifications to our results for very small crystallite sizes that might be relevant to high surface area materials such as those used in catalytic and other applications.

2. Lattice calculations

The calculations presented here refer to a dilute solution of Ca^{2+} in MgO. They are of three types and correspond to calcium substitution in a variety of bulk and surface configurations. We have examined in detail the substitution of single ions, {1 1 0} dimers, {1 1 0} trimers, planar pentamers and complete (infinite) planes of Ca^{2+} ions in the bulk and at the {0 0 1} and {1 1 0} surfaces of MgO using atomistic simulation procedures described in full elsewhere [25]. As on previous occasions [19–23] our approach is based on defect lattice methods developed by Lidiard and Norgett [26] and Norgett [27, 28] for bulk defects and extended to surfaces by Stewart and Mackrodt [19], Mackrodt and Stewart [20] and Tasker [21–23]. We note, in particular, simulation methods employing two-dimensional periodic boundary conditions [21–23] used for whole arrays of substituted ions which saturate the surface region. From this we obtain an energy of substitution appropriate to the limit of high surface segregation. Throughout we employ an ionic model of MgO in which cations and anions have formal charges of +2 and −2 respectively. This has been justified for oxides of this type previously on experimental grounds [29] and confirmed by *ab initio* quantum mechanical cluster calculations [30].

We have used two sets of interatomic potentials, both of which incorporate the shell model introduced by Dick and Overhauser [31] and used subsequently by numerous authors. The first set of potentials is identical to that used previously [24] and is derived from modified electron-gas calculations [32]. Numerical details of these are given in a recent compilation by Colbourn *et al.* [33]. A particular advantage of this approach is that impurity interactions are calculated in exactly the same way as those for the host lattice so that there is a measure of internal consistency about these potentials although they are, of course, approximate. Shell parameters, on the other hand, are obtained empirically by fitting to the observed dielectric constants; the potentials as a whole, therefore, are best described as semi-empirical. The second set of potentials we have used is that obtained by Sangster and Stoneham [34] by fitting to the observed elastic and phonon data in addition to the cohesive energy and lattice constant. Unlike the first set, it is entirely empirical. However, a notable feature of these potentials is that they were derived as a set for a range of rocksalt-structured oxides, including MgO and CaO, assuming a transferable oxygen–oxygen interaction. They are particularly suitable, therefore, in impurity studies. As before, shell parameters are derived by fitting to dielectric data. As discussed previously [35] the two sets of potentials differ in many respects, principally with regard to short-range interactions involving O^{2-} and oxygen polarizability: however, these differences allow us to assess the importance of potentials in calculations such as these.

3. The statistical mechanical model

Previous calculations [36] have applied a monolayer model to minimize the free energy of segregation: the change in entropy of mixing due to segregation is offset by the gain in energy of the segregating species. The model we use here is basically similar in that we identify only two types of site, namely interface and bulk, and include the configurational entropy of the system. Our expressions are generalized for more than two components, and can be evaluated for high surface area materials where it cannot be assumed that the bulk composition is unperturbed by surface segregation.

We write the free energy G, as

$$G = \sum_i n_i^b g_i^b + \sum_i n_i^s g_i^s - kT \ln \Omega \qquad (1)$$

where n_i^b is the number of ions of species i in the bulk of the crystal, n_i^s the corresponding number at the surface (or any other interface) k is Boltzmann's constant and T is the absolute temperature. g_i^b and g_i^s are the individual free energies of the ions, so that Equation 1 neglects interaction terms other than those explicitly included in the calculation of g_i, which are concentration dependent. Ω, the configurational entropy is given by,

$$\Omega = \frac{N_b!}{\left(\prod_i n_i^b!\right)} \frac{N_s!}{\left(\prod_i n_i^s!\right)} \qquad (2)$$

in which N_b and N_s are the number of bulk and surface sites respectively in the crystal. As mentioned earlier, we have assumed that only two types of site need be considered.

Minimizing the total free energy, G, with respect to n_i^b and n_i^s, subject to the constraints,

$$\sum_i n_i^b = N_b = \text{constant}$$
$$\sum_i n_i^s = N_s = \text{constant} \quad (3)$$

and

$$n_i^b + n_i^s = n_i = \text{constant}$$

we get

$$n_i^s/n_i = 1/[1 + \exp(g_i^s - g_i^b - \lambda)/kT] \quad (4)$$

The constraints (Equation 3) make the number of bulk and surface sites independently constant. The model does not, therefore, allow for restructuring of the surface in a way that depends on the degree of segregation if that restructuring alters the density of surface sites. The Lagrange multiplier, λ, is given by

$$\sum_i n_i/[1 + \exp(g_i^s - g_i^b - \lambda)/kT] = N_s \quad (5)$$

or alternatively

$$\sum_i n_i/[1 + \exp(g_i^b - g_i^s + \lambda)/kT] = N_b \quad (6)$$

For a two-component system, the experimentally measured quantity is usually n_1^s/n_2^s, which is given by

$$\frac{n_1^s}{n_2^s} = \frac{n_1}{n_2} \frac{[1 + \exp(g_2^s - g_2^b - \lambda)/kT]}{[1 + \exp(g_1^s - g_1^b - \lambda)/kT]} \quad (7)$$

When $N_s \ll n_i$, *for all* i, Equation 5 reduces to

$$\lambda = -kT \ln\left[\sum_i \frac{n_i}{N_s \exp(g_i^s - g_i^b)/kT}\right] \quad (8)$$

This condition will hold for macroscopic crystals with any measurable level of impurity. Substituting for λ in Equation 7 and simplifying we obtain the usual simple Arrhenius expression,

$$n_1^s/n_2^s = f \exp(-H/kT) \quad (9)$$

in which f is the impurity concentration or doping level,

$$f = n_1/n_2 \quad (10)$$

and H is given by

$$H = (g_1^s - g_1^b) - (g_2^s - g_2^b) \quad (11)$$

If the changes in vibrational entropy on segregation can be neglected, we can associate the free energies, g_i, with the substitutional energies derived from our static lattice calculation. Thus,

$$g_1^s - g_2^s = \Delta E^s$$

and

$$g_1^b - g_2^b = \Delta E^b \quad (12)$$

where ΔE^s and ΔE^b are the substitutional energies of ion 1 for ion 2 in the surface and bulk, respectively. Hence,

$$H = \Delta E^s - \Delta E^b \quad (13)$$

H, therefore, is equal to the enthalpy of segregation, which is obtained from experiment via the Arrhenius relationship, Equation 9.

In the derivation given above, we have shown how substitutional energies obtained from static lattice calculations give an enthalpy of segregation, which for macroscopic crystals, leads to an Arrhenius temperature dependence for the surface concentrations. For small crystallites ($N_s \sim n_i$) an explicit evaluation of Equations 4 and 5 gives the dependence on crystal size. Calculations described in the following section show that the substitutional energies (per ion), ΔE^s and ΔE^b, are dependent on the degree of segregation through defect interactions. This we accommodate in our theory by choosing values appropriate to the high degree of segregation predicted, thereby including impurity interaction terms.

4. Results

Magnesium oxide and calcium oxide both have the rocksalt (f c c) structure and the solution of one in the other occurs by cation substitution. For the reaction,

$$CaO + Mg_{Mg}^{2+} \rightleftharpoons Ca_{Mg}^{2+} + MgO$$

the heat of solution, ΔH_{soln}, is given by

$$\Delta H_{soln} = \Delta E^b - W_L(CaO) + W_L(MgO) \quad (14)$$

where $W_L(CaO)$ and $W_L(MgO)$ are the appropriate cohesive energies and ΔE^b the energy to substitute Ca^{2+} in MgO, including lattice relaxation. The calculated values for these quantities derived from the two potentials we use are recorded in Table I. The theoretical estimates are similar and the calculated cohesive energies agree well with experiment.

TABLE I Calculated bulk and surface properties of MgO obtained using two different interionic potentials. Comparison with experiment is shown. The calculated enthalpy of solution neglects volume changes on substitution and is obtained from Equation 14

	Non-empirical potentials	Empirical potentials	Experiment
Cohesive energy CaO(eV)	−36.4	−36.0	−36.0 [21]
Cohesive energy MgO(eV)	−40.8	−41.0	−40.4 [21]
Substitutions energy Ca^{2+}_{Mg}(eV)	5.82	6.52	
Enthalpy of solution (eV)	1.42	1.52	
Surface energy {001} (Jm^{-2})	1.1	1.2	1.04, 1.2, 1.15 [22]
Surface energy {110} (Jm^{-2})	2.9	2.9	

The predominant (lower energy) surface of fcc materials has a {001} orientation, and this we have examined in detail for direct comparison with experiment. For completeness, however, we also present results for the {110} surface. Surface energies derived from the two potentials are also given in Table I. Again, there is close agreement between the two models, and with experiment. Surfaces of this type generally show a slight rumpling, with outward movement of anions and inward cation displacements. Both experiment [37–39] and theory [19, 20] show this to be very small in MgO and CaO and the present calculations support this view. Thus we believe our *non-defective* surfaces, which form the basis of any segregation calculation, to be a fairly accurate model for real *planar* surfaces in MgO.

In Tables II and III we have summarized our calculated substitution energies for Ca^{2+} near a {001} surface of MgO, based on electron-gas and empirical potentials respectively. We have considered clusters of one to five ions building up to a saturated plane in the surface layer, one layer below the surface and in the bulk. The results shown are for a single ion, a trimer of ions oriented along the {110} direction, a square array of five calcium ions and a complete plane. An initial aggregation of ions in the {110} direction produces a small reduction in the substitution energy *per ion* by virtue of elastic relaxation of the type previously discussed [24], but as the aggregates grow we observe a small increase in energy due to the mutual repulsion of the larger ions. In the bulk, the energy per ion for a complete plane is ~ 0.2 eV higher than for an isolated substitute due to these repulsions. In the surface, the additional energy for aggregation is somewhat greater. We note, in particular, that the energy for complete planes of Ca^{2+} ions varies very little with distance from the surface until the surface layer itself. This provides additional justification for our thermodynamic model of segregation outlined in Section 3. Our results based on empirical potentials confirm those found previously [24] in that both predict substitution energies for single ions at the surface which are substantially lower than for the bulk, thereby indicating a strong tendency for segregation. This is the usual result for large ions substituting for smaller host ions and is due to the relief of elastic strain [24]. However, despite the increase in substitution energy with aggregation, a saturated plane still has a lower energy at the surface than in the bulk. We conclude from this that at absolute zero the equilibrium segregation of Ca^{2+} in MgO would lead to a saturated layer and the remaining solute dispersed as isolated point defects in the bulk. As mentioned before, we find some evidence that {110} dimers and trimers may

TABLE II Energies (eV) per substituted calcium ion for clusters on {001} planes near an MgO surface calculated using non-empirical potentials

	Single subsitution $1 \times Ca^{2+}$	(110) Dimer $2 \times Ca^{2+}$	(110) Trimer $3 \times Ca^{2+}$	Planar $5 \times Ca^{2+}$	Complete plane of Ca^{2+} $\infty \times Ca^{2+}$
Plane 1 (surface layer)	3.54	3.57	3.56	3.63	4.20
Plane 2	4.61	4.59	4.54	4.61	4.74
Plane 3	–	–	–	–	4.72
Bulk	4.62	4.60	4.62	4.71	4.72

TABLE III Energies (eV) per substituted calcium ion for clusters on {001} planes near an MgO surface calculated using empirical potentials

	Single substitution $1 \times Ca^{2+}$	(110) Dimer $2 \times Ca^{2+}$	(110) Trimer $3 \times Ca^{2+}$	Planar $5 \times Ca^{2+}$	Complete plane $\infty \times Ca^{2+}$
Plane 1 (surface plane)	4.82	4.88	4.88	4.88	5.74
Plane 2	6.44	–	6.13	6.35	6.66
Plane 3	–	–	–	–	6.64
Bulk	6.52	–	6.57	6.64	6.65

be stable in the bulk, but the binding energies are thought to be small.

From our calculated substitution energies we deduce enthalpies of segregation, given by Equation 13, in the limit of high segregation. They are given by: (a) electron-gas potentials

$$H = (4.20 - 4.62)\,\text{eV} = -0.42\,\text{eV}$$

and (b) empirical potentials

$$H = (5.74 - 6.52)\,\text{eV} = -0.78\,\text{eV}$$

At very high temperatures, when there is little segregation, the interaction between Ca_{Mg}^{2+} ions is less and the enthalpies of segreagation decrease to -1.08 and -1.70 eV respectively for the two potentials. Taking the high segregation enthalpies and a concentration of calcium in magnesia of 220 ppm, the Arrhenius expression of Equation 9 gives the temperature dependence of Ca^{2+} surface concentration shown in Fig. 1. These are exactly the experimental conditions under which Wynblatt and McCune have examined this system recently [17]. Using Auger electron spectroscopy to determine surface concentrations they deduce a heat of segregation of -0.78 ± 0.22 eV. Our results are in good agreement with this value, particularly so for those derived from empirical potentials. Our Arrhenius plot has the same gradient as experiment [17], but the concentrations at each temperature are approximately six times greater. Theory and experiment can be brought into better agreement if one assumes that the AES technique samples, and hence averages, over the first few atomic layers. A further discrepancy is that our calculations have also neglected the effects of dispersing the segregated species over a few layers at finite temperatures.

In Table IV we summarize our results for the {110} surface. Once again we find a strong tendency for the larger Ca^{2+} ion to segregate at the surface. In this case, however, the lattice environment, as reflected in the substitution energies, does not reach that of the bulk till approximately the sixth layer into the crystal.

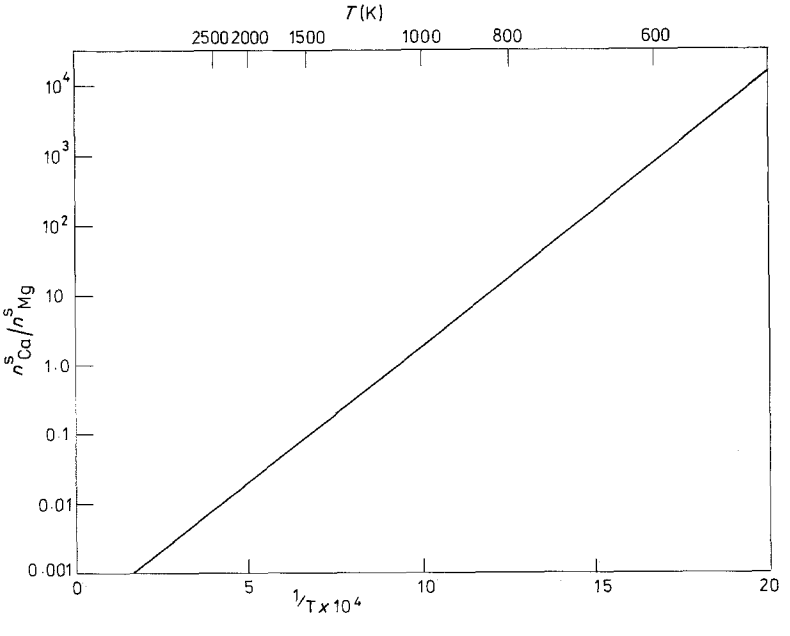

Figure 1 The calculated ratio of calcium to magnesium ions in the {001} surface layer of MgO containing 220 ppm of calcium as a function of temperature. The enthalpy of segregation is taken as -0.78 eV.

TABLE VI Energies (eV) of substitution per Ca^{2+} ion near a {110} MgO surface

	Calculated potentials		Empirical potentials	
	Single substitution $1 \times Ca^{2+}$	Complete plane $\infty \times Ca^{2+}$	Single substitution $1 \times Ca^{2+}$	Complete plane $\infty \times Ca^{2+}$
Plane 1 (surface plane)	3.19	3.86	3.97	4.86
Plane 2	5.14	5.06	5.29	6.78
Plane 3	4.40	4.40	–	6.08
Plane 4	–	4.65	–	6.36
Bulk	4.62	–	6.52	–

Furthermore, the substitution energy in the plane just below the surface is somewhat higher than in the bulk; and this is quite a different situation to that at the {001} surface. Our simple monolayer model for the temperature dependence, therefore, is unlikely to be adequate here.

Quantitative measurements have also been made for the MgO–NiO system by Cimino *et al.* [18]. Previous calculations [19, 20] based on empirical potentials similar to those used here have given substitution energies for isolated Ni^{2+} ions in the bulk and at the {001} surface. From these values we estimate an enthalpy of segregation of approximately + 0.01 eV which agrees well with the observation [18] that there is no appreciable deviation from bulk composition for this system except for a possible slight depletion of Ni^{2+} ions at the surface.

5. Small crystallites

Our simple model outlined in Section 3 is based on macroscopic crystals. However, many important surface phenomena involve very high surface area materials and hence small crystallite size. In these circumstances, the Arrhenius expression of Equation 9 is no longer valid since $N_s \sim n_i$, as opposed to $N_s \ll n_i$ which is the case for large particles. However, the degree of segregation can still be calculated from Equations 4 and 5 without further approximation. The result depends only on the enthalpy of segregation, H, as defined by Equation 11 for a two-component system, and can be seen most easily if we write

$$y = \exp(g_2^s - g_2^b - \lambda)/kT \qquad (15)$$

Equation 4 then takes the form,

$$\frac{n_1^s}{n_1} = \frac{1}{1 + \exp(H/kT)y} \qquad (16)$$

while y is determined from Equation 5, which we now write as

$$\frac{n_1}{1 + \exp(H/kT)y} + \frac{n_2}{1 + y} = N_s \qquad (17)$$

Fig. 2 shows the fraction of surface sites, n_1^s/N_s,

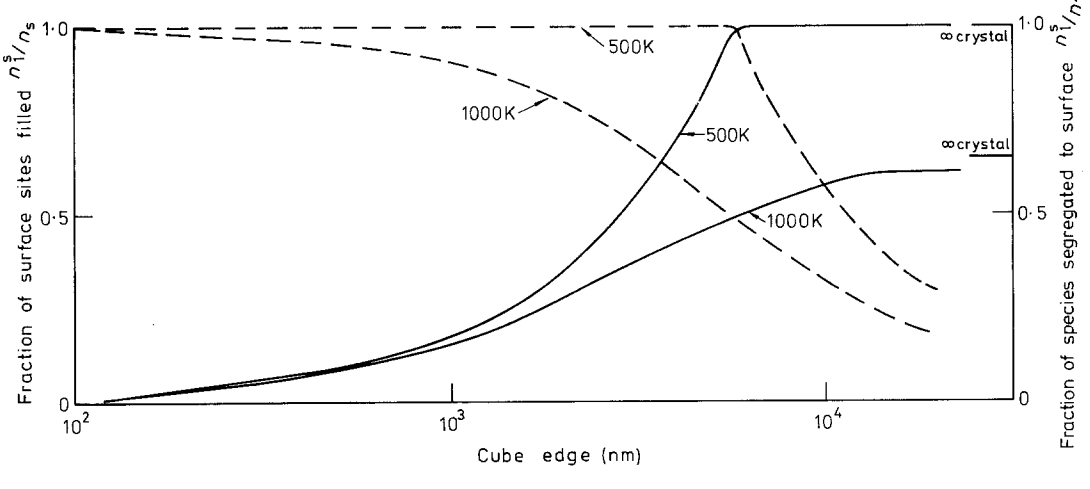

Figure 2 Solid curve: the fraction of {001} surface sites in MgO occupied by calcium ions given for two temperatures and a total calcium concentration of 220 ppm. Broken curve: the fraction of the impurity calcium ions that are in the surface layer for the same temperature and concentration.

occupied by calcium ions as a function of crystallite size at 500 and 1000 K. In calculating n_1^s/N_s we have assumed cubic crystallites, a calcium concentration of 220 ppm and a value of -0.78 eV for H. Also shown in Fig. 2 are the large (∞) crystal values for n_1^s/N_s: they are 1.0 and 0.65 at 500 and 1000 K, respectively. Even at the lower temperature the surface is not saturated until the crystal size is approximately 10 μm, while at 1000 K particles of this size have not reached the large crystal equilibrium value of 0.65. The significance of these results is that many catalytic processes, for example, utilize crystallite sizes substantially less than 10 μm so that impurity segregation in these systems will differ appreciably from that in coarser-grained materials.

Also shown in Fig. 2 (as broken lines) is the fraction of calcium ions in the surface, n_1^s/n_1, at the same two temperatures: the remainder, $n_1 - n_1^s$, is distributed in the bulk. At 500 K when surface segregation, as opposed to saturation, is almost complete, the effects of crystal size can be seen quite clearly. Small crystals, as distinct from macroscopic material, possess *relatively* large numbers of surface sites and this leads to less saturation of the surface simply because there are insufficient impurity ions to fill these sites. There will be a tendency for all impurity ions to fill surface sites up to saturation and then to occupy the bulk. The net effect of this is that the bulk concentration will not reach the infinite or large crystal value until particle sizes exceed about 100 μm. We suggest, therefore, that this rather simple geometric factor, namely surface to bulk ratio, will have a substantial influence on the relative behaviour of small and large crystals. At high temperature the situation is less extreme with impurity ions filling both bulk and surface sites at almost all crystal sizes. However, crystals need to be in excess of ~ 100 μm before the bulk concentration approaches the total impurity level.

6. Conclusions

This paper has attempted to give a theoretical description of the segregation of calcium ions at the surface of magnesium oxide. From the results presented we conclude that simple (ideal solution) statistical mechanical considerations can be combined with detailed atomistic lattice simulation to give a quantitative prediction of surface segregation. Furthermore, the treatment of defect clusters and complete planes of impurity ions in our atomistic calculations enables the present results to be extended beyond the ideal solution approximation, since impurity–impurity interaction terms have been included explicitly. For two-component systems we demonstrate that Arrhenius behaviour applies only to macroscopic crystals, while microcrystallites show substantially modified characteristics. In particular, we suggest that the increased surface to bulk site ratio for small crystals will lead to less saturation and a greatly reduced bulk concentration of impurity by comparison with macroscopic material. In the specific case of calcium in magnesium oxide we find a strong tendency towards segregation at the surface and calculate enthalpies of -0.42 and -0.78 eV for the two potentials we have used. The latter, in particular, which derives from recent empirical potentials [35], is in good agreement with recent Auger electron spectroscopy results [17]. The two site model we have used together with the assumption of a simple planar surface is clearly a gross approximation; however, the results presented here suggest that it might provide a useful starting point for the theoretical investigation of surface segregation.

Acknowledgements

We should like to thank Dr A. B. Lidiard for valuable advice on the thermodynamics of surface segregation and Dr P. T. Greenland for useful discussions.

References

1. J. FRENKEL, "Kinetic Theory of Liquids" (Dover, New York, 1948).
2. K. LEHOVEC, *J. Chem. Phys.* **21** (1953) 1123.
3. Y. T. TAN, *Prog. Solid State Chem.* **10** (1976) 193.
4. K. L. KLIEWER and J. S. KOEHLER, *Phys. Rev.* **140A** (1965) 1226.
5. W. D. KINGERY, *J. Amer. Ceram. Soc.* **57** (1974) 1.
6. *Idem, ibid.* **57** (1974) 74.
7. W. C. JOHNSON, D. F. STEIN and R. W. RICE, in "Grain Boundaries in Engineering Materials" edited by J. C. Walter, J. H. Westbrook and D. A. Woodford (Claitors Publishing Division, Baton Rouge La., 1975).
8. W. D. KINGERY, T. MITAMURA, J. B. VANDER SANDE and E. L. HALL, *J. Mater. Sci.* **14** (1979) 1766.
9. T. MITAMURA, E. L. HALL, W. D. KINGERY and J. B. VANDER SANDE, *Ceramurgia Int.* **5** (1979) 131.

10. J. R. BLACK and W. D. KINGERY, *J. Amer. Ceram. Soc.* **62** (1979) 176.
11. C. BERTHELET, W. D. KINGERY and J. B. VANDER SANDE, *Ceramurgia Int.* **2** (1976) 62.
12. W. D. KINGERY, W. L. ROBBINS, A. F. HENRIKSEN and C. E. JOHNSON, *J. Amer. Ceram. Soc.* **59** (1976) 239.
13. M. W. ROBERTS and R. St. C. SMART, *Chem. Phys. Lett.* **69** (1980) 234.
14. *Idem, Surf. Sci.* **100** (1980) 590.
15. *Idem, Surf. Sci.* **108** (1981) 271.
16. W. C. JOHNSON and J. M. BLAKELY (eds), "Interfacial Segregation" (American Society for Metals, Ohio, 1979).
17. P. WYNBLATT and R. C. McCUNE, in "Surfaces and Interfaces in Ceramic and Ceramic Metal Systems", edited J. Pask and A. Evans (Plenum Press, New York, 1981).
18. A. CIMINO, B. A. De ANGELIS, G. MINELLI, T. PERSINI and P. SCARPINI, *J. Solid State Chem.* **33** (1980) 403.
19. R. F. STEWART and W. C. MACKRODT, *J. Phys.* **C7** (1976) 247.
20. W. C. MACKRODT and R. F. STEWART, *ibid.* **C10** (1977) 1431.
21. P. W. TASKER, *Phil. Mag.* **A39** (1979) 119.
22. *Idem, Surf. Sci.* **87**, (1979) 315.
23. P. W. TASKER, in "Computer Simulation of Solids", edited by C. R. A. Catlow and W. C. Mackrodt (Springer-Verlag, Berlin, 1982).
24. E. A. COLBOURN and W. C. MACKRODT, *J. Mater. Sci.* **17** (1982) 3021.
25. C. R. A. CATLOW and W. C. MACKRODT, in "Computer Simulation of Solids", edited by C. R. A. Catlow and W. C. MACKRODT (Springer-Verlag, Berlin, 1982).
26. A. B. LIDIARD and M. J. NORGETT, in "Computational Solid State Physics", edited by F. H. Herman, N. W. Dalton and T. R. Koehler (Plenum Press, New York, 1972).
27. M. J. NORGETT, AERE Report R.7015 (1972).
28. Idem, AERE Report R.7605 (1974).
29. C. R. A. CATLOW, W. C. MACKRODT, M. J. NORGETT and A. M. STONEHAM, *Phil. Mag.* **35** (1977) 177.
30. E. A. COLBOURN and W. C. MACKRODT, submitted for publication (1983).
31. B. G. DICK and A. W. OVERHAUSER, *Phys. Rev.* **112** (1958) 90.
32. W. C. MACKRODT and R. F. STEWART, *J. Phys.* **C12** (1979) 431.
33. E. A. COLBOURN, J. KENDRICK and W. C. MACKRODT, ICI Corporate Laboratory Report CL-R/81/1657/A (1981).
34. M. J. L. SANGSTER and A. M. STONEHAM, *Phil. Mag.* **B43** (1981) 597.
35. C. R. A. CATLOW, M. DIXON and W. C. MACKRODT, in "Computer Simulation of Solids", edited by C. R. A. Catlow and W. C. Mackrodt (Springer-Verlag, Berlin, 1982).
36. S. Y. LIU and H. H. KUNG, *Surf. Sci.* **110** (1981) 504.
37. C. G. KINNIBURGH, *J. Phys.* **C8** (1975) 2382.
38. M. PRUTTON, J. A. WALKER, M. R. WELTON-COOK, R. C. FELTON and J. A. RAMSEY, *Surf. Sci.* **89** (1979) 95.
39. T. GOTOH, S. MURAKAMI, K. KINOSITA and Y. MURATA, *J. Phys. Soc. Jpn.* **50** (1981) 2063.
40. G. V. SAMSONOV, "The Oxide Handbook" (IFI/Plenum, New York, 1973).
41. M. P. TOSI, *Solid State Phys.* **16** (1964) 1.

Received 15 July
and accepted 20 September 1982